DOI: 10.21122/2220-9506-2026-17-1-23-30

Optimization of the Optical Measuring Converter's Geometric Properties for the Microelectromechanical Pressure Sensor

E.S. Barbin[1], T.G. Nesterenko[1,2], P.F. Baranov[2], D.P. Ilyaschenko[2], S.E. Vtorushin[1], A.A. Talovskaya[1], D.M. Mokhovikov[1], A.N. Koleda[1,2], A. Myrzakhmetov[1]

[1]*Tomsk State University of Control Systems and Radioelectronics, Lenin Ave., 40, Tomsk 634034, Russia*

[2]*National Research Tomsk Polytechnic University, Lenin Ave., 30, Tomsk 634050, Russia*

Received 27.10.2025
Accepted for publication 29.12.2025

Abstract

Nowadays development and production of microelectromechanical systems is one of the most promising directions in the world's economy. One of the innovative fields in the development of microsystems is integration of optical devices as measuring transducers. Goal of the paper is optimization of the optical measuring transducer geometry for microelectromechanical pressure sensor which provides a required value and linearity of the optical transmission coefficient. Microelectromechanical pressure sensor comprises the optical measuring transducer represented by a pair of waveguides that form an optical directional coupler. Linearity of the optical transmission coefficient of the transducer is provided by the selection of the initial gap between the waveguides at the linear section of the curve representing dependence of the optical transmission coefficient on the gap. Calculation of the required characteristics of such transducer requires a combination of the Finite-difference time-domain method and the mode overlapping method. This allows calculating the magnitude of the optical transmission coefficient for different geometric parameters of the transducer. Two models of the directional coupler with silicon and silicon nitride waveguides were used to determine dependencies of the transducer's optical transmission coefficient on the optical coupling length and the waveguide bending radius. The data obtained were used to plot the dependencies of the transmission coefficient on the gap between the waveguide for both models. The plots show the optimal initial gaps and the length of the linear section. The results allow designing a device with predetermined working section at which the optical measuring transducer can measure membrane displacements that are linearly proportional to an acting pressure. Such working section is characterized by the initial gap in the middle of the linear section that amounts to 500 nm for silicon waveguides and 600 nm for silicon nitride ones. The linear section of the transducer's transmission characteristic for the waveguides of both types is estimated as ±80 nm in relation to the initial gap. In this section, the optical transmission coefficient of the transducer with silicon waveguides alters from 0 to 0.86 which corresponds to a value of $5.375 \cdot 10^6$ m^{-1}. For the waveguide with silicon nitride waveguides the coefficient varies from 0.09 to 0.53 which corresponds to a value of $2.75 \cdot 10^6$ m^{-1}. The computer aided analysis methods allow for determining the optimal geometry of the evanescent coupling-based measuring transducer that is used in the microelectromechanical pressure sensor. The presented models of two transducers with two waveguides made of different materials demonstrate different characteristics. The optimal parameters for each of the models are achieved at different waveguide bending radii and optical coupling lengths.

Keywords: evanescent coupling, optical waveguides, directional coupler, coupling length, transmission coefficient

Адрес для переписки:
Барбин Е.С.
National Research Tomsk Polytechnic University,
пр-т Ленина, 30, г. Томск 634050, Россия
e-mail bar_es@mail.ru

Address for correspondence:
Barbin E.S.
National Research Tomsk Polytechnic University,
Lenin Ave., 30, Tomsk 634050, Russia
e-mail bar_es@mail.ru

Для цитирования:
Е.С. Барбин, Т.Г. Нестеренко, П.Ф. Баранов, Д.П. Ильященко, С.Е. Вторушин, А.А. Таловская, Д.М. Моховиков, А.Н. Коледа, А. Мырзахметов.
Оптимизация геометрических характеристик оптического измерительного преобразователя микроэлектромеханического датчика давления.
Приборы и методы измерений.
2026. Т. 17. № 1. С. 23-30.
DOI: 10.21122/2220-9506-2026-17-1-23-30

For citation:
Barbin ES, Nesterenko TG, Baranov PF, Ilyaschenko DP, Vtorushin SE, AA Talovskaya, DM Mokhovikov, AN Koleda, Myrzakhmetov A.
Optimization of the Optical Measuring Converter's Geometric Properties for the Microelectromechanical Pressure Sensor.
Devices and Methods of Measurements.
2026;17(1):23-30.
DOI: 10.21122/2220-9506-2026-17-1-23-30

DOI: 10.21122/2220-9506-2026-17-1-23-30

Оптимизация геометрических характеристик оптического измерительного преобразователя микроэлектромеханического датчика давления

Е.С. Барбин[1], Т.Г. Нестеренко[1,2], П.Ф. Баранов[2], Д.П. Ильященко[2], С.Е. Вторушин[1], А. А. Таловская[1], Д.М. Моховиков[1], А.Н. Коледа[1,2], А. Мырзахметов[1]

[1]Томский государственный университет систем управления и радиоэлектроники, пр-т Ленина, 40, г. Томск 634034, Россия
[2]Национальный исследовательский Томский политехнический университет, пр-т Ленина, 30, г. Томск 634050, Россия

Поступила 27.10.2025
Принята к печати 29.12.2025

В настоящее время разработка и производство микроэлектромеханических систем является одним из наиболее перспективных направлений развития мировой экономики. Одним из инновационных направлений в развитии микросистемной техники является интеграция оптических устройств в качестве измерительных преобразователей. Целью данной работы являлась оптимизация геометрии оптического измерительного преобразователя микроэлектромеханического датчика давления для обеспечения требуемой величины и линейности оптического коэффициента передачи. Микроэлектромеханический датчик давления содержит оптический измерительный преобразователь в виде пары волноводов, образующих оптический направленный ответвитель. Линейность оптического коэффициента передачи преобразователя обеспечивалась выбором оптимального начального зазора между волноводами на линейном участке кривой зависимости оптического коэффициента передачи от зазора. Для расчёта требуемых характеристик такого преобразователя использовалась комбинация метода конечных разностей во временной области и метода перекрытия мод. Это позволило рассчитать величину оптического коэффициента передачи при различных геометрических параметрах преобразователя. Используя две модели направленного ответвителя с кремниевыми и нитрид-кремниевыми волноводами были определены зависимости величины оптического коэффициента передачи преобразователя от длины оптической связи и радиуса изгиба волноводов. Используя полученные данные, для обеих моделей построены зависимости коэффициента передачи от зазора между волноводами, где были показаны оптимальные величины начальных зазоров и диапазон линейного участка. Проведённые в данной работе исследования позволили на этапе проектирования определить рабочий участок, на котором оптический измерительный преобразователь может измерять перемещения мембраны, пропорциональные действующему давлению в линейном диапазоне. Такой рабочий участок характеризуется начальным зазором в середине линейного участка, который составляет 500 нм для кремниевых волноводов и 600 нм для нитрид-кремниевых. При этом линейный участок передаточной характеристики преобразователя для обоих типов волноводов оценивается в ±80 нм относительно начального зазора. В этом диапазоне оптический коэффициент передачи преобразователя с кремниевыми волноводами меняется в диапазоне от 0 до 0,86, что соответствует величине $5{,}375 \cdot 10^6$ м$^{-1}$. Диапазон изменения коэффициента передачи преобразователя с нитрид-кремниевыми волноводами лежит в пределах от 0,09 до 0,53, что соответствует величине $2{,}75 \cdot 10^6$ м$^{-1}$. Использованные методы компьютерного анализа позволили определить оптимальные геометрические характеристики оптического измерительного преобразователя, основанного на эффекте оптического туннелирования, используемого в микроэлектромеханическом датчике давления. Представленные модели преобразователей с волноводами из двух различных материалов показали различие по своим характеристикам. Оптимальные параметры для каждой модели достигаются при различных радиусах изгиба волноводов и длинах оптической связи.

Ключевые слова: оптическое туннелирование, оптические волноводы, направленный ответвитель, длина связи, коэффициент передачи

Адрес для переписки:
Барбин Е.С.
National Research Tomsk Polytechnic University,
пр-т Ленина, 30, г. Томск 634050, Россия
e-mail bar_es@mail.ru

Address for correspondence:
Barbin E.S.
National Research Tomsk Polytechnic University,
Lenin Ave., 30, Tomsk 634050, Russia
e-mail bar_es@mail.ru

Для цитирования:
Е.С. Барбин, Т.Г. Нестеренко, П.Ф. Баранов, Д.П. Ильященко, С.Е. Вторушин, А.А. Таловская, Д.М. Моховиков, А.Н. Коледа, А. Мырзахметов.
Оптимизация геометрических характеристик оптического измерительного преобразователя микроэлектромеханического датчика давления.
Приборы и методы измерений.
2026. Т. 17. № 1. С. 23-30.
DOI: 10.21122/2220-9506-2026-17-1-23-30

For citation:
Barbin ES, Nesterenko TG, Baranov PF, Ilyaschenko DP, Vtorushin SE, AA Talovskaya, DM Mokhovikov, AN Koleda, Myrzakhmetov A.
Optimization of the Optical Measuring Converter's Geometric Properties for the Microelectromechanical Pressure Sensor.
Devices and Methods of Measurements.
2026;17(1):23-30.
DOI: 10.21122/2220-9506-2026-17-1-23-30

Introduction

Currently microelectromechanical (MEMS) pressure sensors are highly needed in the oil & gas and automotive industries, control systems of space vehicles and launch site ground facilities, in steam and gas turbines to control pressure fluctuations and measure dynamic pressure at high temperatures, in atomic reactors, personalized medicine or smart home systems. Increased accuracy and sensitivity of pressure sensors (capability of detecting small pressure fluctuations) allow for early identification of industrial and natural emergency situations. Depending on the application field the sensors can be capacitive, piezoelectric, tensoresistive and of other types described elsewhere [1–5]. However the resolution and minimal sensitivity threshold of such sensors is mainly limited by the design concept of the transducers [6–9]. The destabilizing factors (capacitive couplings, temperature, electromagnetic impacts, etc.) can be compensated by advanced design and manufacturing techniques. An ideal variant is to put all the electronic components in a single package together with the MEMS transducer.

Another promising type of transducers are optical pressure sensors [10–13]. The most widely spread are optical fiber sensors implementing fiber Bragg gratings. Such sensors provide high noise resistance, fire safety and immunity to electromagnetic noise. This is conditioned by the fact that optical signal modulation requires small exposure on the section with the Bragg grating, irrespective of it to be mechanical or thermal.

However this fact induces major impediments to the application of Bragg grating-based transducers in high-precision measurements. Therefore, further miniaturization and cost reduction of optical pressure sensor fabrication require novel types of transducers possessing the advantages of optical methods, while lacking some of their drawbacks. The most promising integral transducer for the pressure sensor is evanescent coupling-based transducer. It requires no complex scheme of output signal processing and expensive equipment, while having lesser sensitivity to temperature change. Moreover, electromagnetic noise has no impact on the transmission of optical signal from a radiation source to the photosensitive element [14].

Aim of this work was determining the optimal characteristics of the newly developed evanescent coupling-based measuring transducer for a MEMS pressure sensor using computer simulation methods. This will enable the creation of a pressure sensor with integrated packaging of the sensor's components (electronics, laser and photodiode) in a single case, which vastly expands the application field of such measuring transducers.

Functional scheme of the pressure sensor

Integrated optical pressure sensor is an microoptoelectromechanical system which functional scheme is given in Figure 1. The sensing element of the pressure sensor contains bottom wafer with membrane 1 and top wafer 2 coupled by stoppers 3 intended for the formation of initial air gap G_0. Both wafers comprise bottom 4 and top 5 optical integrated waveguides surrounded by silicon oxide layers 6. Optical waveguides 4 and 5 form the optical measuring transducer (OMT) implemented as a directional coupler. Optical radiation from a laser diode is fed into bottom waveguide 4 with optical power Popt in, that at working gap G_0 flows into top waveguide 5 with power $P_{opt\ dis} = 0.5 \cdot P_{opt\ in}$ and consequently dissipates. The output optical signal from the sensor's' sensing element with power $P_{opt\ out}(P)$ hits the photodiode and at the output forms $I_{out}(P)$ which is further amplified by the electronic unit with the formation of voltage at the output. Under pressure P, membrane bends, thus changing gap $G(P)$ between waveguides 4 and 5 of the OMT. This alters the optical power at the output of the bottom waveguide

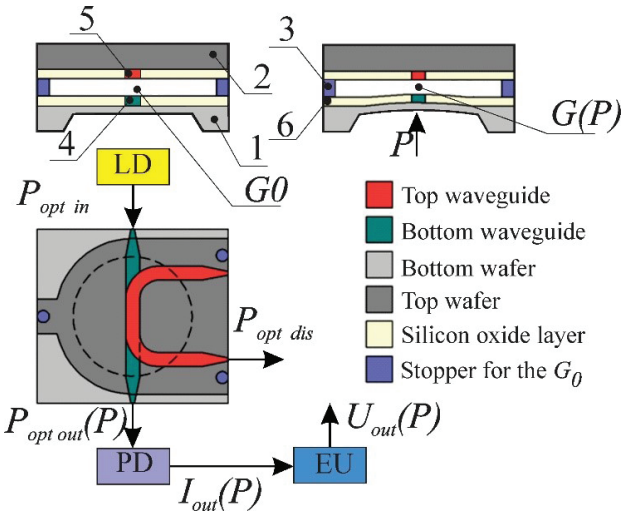

Figure 1 – Functional scheme of the pressure sensor: LD – laser diode; PD – photodiode; EU – electronic unit

$P_{opt\ out}(P)$ proportionally to the membrane bend and, respectively, applied pressure.

Geometric characteristics

To optimize the geometric parameter of the directional couplers, the finite-difference time-domain (FDTD) method was used. This analysis is applicable to three-dimensional objects, which is very resource consuming. Therefore, the number of studied points was much smaller than in the case of two-dimensional analysis by the mode overlapping method in finite difference eigenmode (FDE). The task of the combined analysis by the FDTD and FDE methods was to determine the most optimal investigation route and to build a more accurate mathematical model of the OMT.

The first stage was to analyze and select the parameters of the smooth junction of the OMT's directional coupler. The coupling length L_c in the analysis was minimal and the gap G was preset. The geometry under study is exemplified in Figure 2 by Si_3N_4 waveguides. For the analysis the most useful is the L_{pl}/H_{pl} ratio, rather than the absolute values of the height H_{pl} and length L_{pl}. For Si_3N_4 length L_{pl} reached 30 μm, while for silicon on insulator waveguide (SOI) it was 20 μm. The analysis results are presented in Figures 3 and 4.

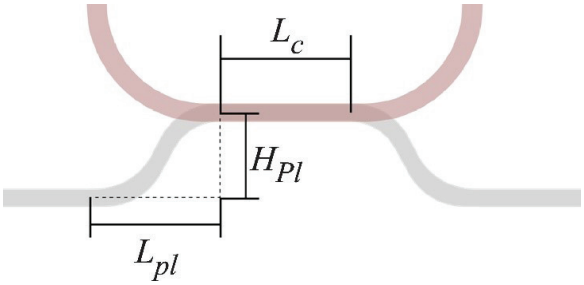

Figure 2 – Geometry of the smooth junction of the optical measuring transducer directional coupler

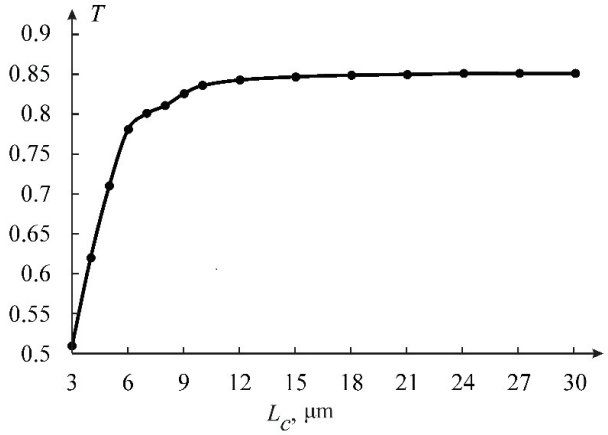

Figure 3 – Dependence of the transmission coefficient on the geometry of the smooth junction for Si_3N_4

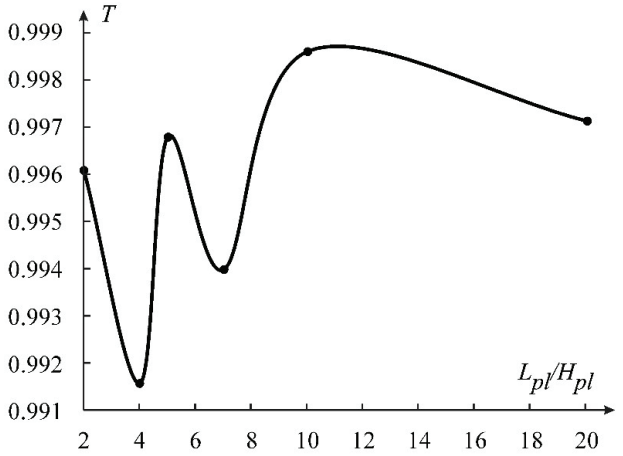

Figure 4 – Dependence of the transmission coefficient on the geometry of the smooth junction for silicon on insulator

Si_3N_4 waveguides with dimensions of 350×1400 nm had calculated losses of about 3 dB/mm and a minimum permissible bending radius of 60 μm. Therefore, high values of H_{pl} caused additional losses at bends. Minimum permissible ratio L_{pl}/H_{pl} amounted to 10, which corresponded to $H_{pl} = 3$ μm and $L_{pl} = 30$ μm. These values were accepted for further modeling.

For silicon waveguide on the SOI wafer with dimensions of 220×550 nm, the bending radius could reach 5 μm, so the smooth junction of the directional coupler had lesser effect on the additional losses as compared to silicon nitride. Minimum permissible ratio L_{pl}/H_{pl} was accepted to be 5, which corresponded to $H_{pl} = 4$ μm and $L_{pl} = 20$ μm.

The FDTD method was used to analyze the effect of the coupling length on the OMT's transmission coefficient at preset gaps (Figures 5 and 6). For 350×1400-nm Si_3N_4 waveguides, the gap amounted to 600 nm; for 220×500-nm SOI waveguides that amounted to 500 nm.

The analysis has shown a considerable effect of the interaction of the waveguides in real geometry which occurred not only in the zone of immediate waveguide interaction, but also in the zone of the smooth junction. At a coupling length of 1 μm, the transmission coefficient with due consideration of all losses amounted to 0.68. Taking into account the results of the smooth junction analysis with maximum transmission coefficient of 0.85, the contribution of a single smooth junction to the total coupling coefficient could be calculated as (0.85-0.68)/2 which amounted to 0.085. Following these results, the calculated length that provided the working point to lie

in the middle of the output signal alteration range at a gap of 600 nm should be equal to 15 μm, which differs from a value of 24 μm obtained by the FDE method.

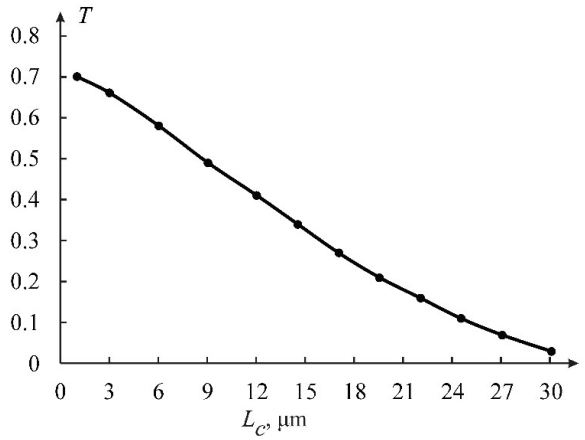

Figure 5 – Dependence of the transmission coefficient on the coupling length L_c at a gap G = 600 nm for Si_3N_4

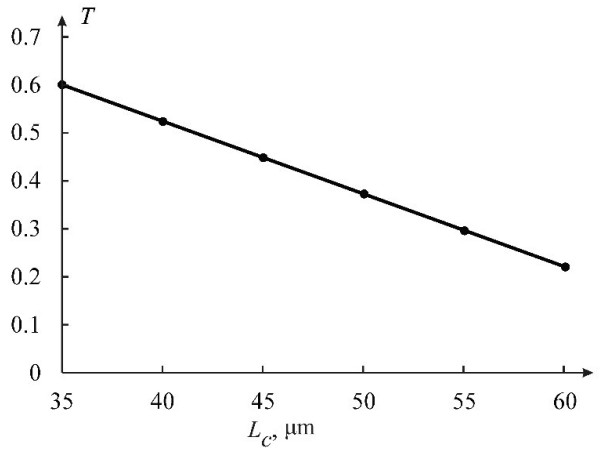

Figure 6 – Dependence of the transmission coefficient on the coupling length L_c at a gap G = 500 nm for silicon on insulator

For the SOI waveguide, at a coupling length of 1 μm, the transmission coefficient with due consideration of all losses amounted to 0.984. Taking into account the results of the smooth junction analysis with maximum transmission coefficient of 0.997, the contribution of a single smooth junction to the total coupling coefficient amounted to (0.997-0.984) / 2 = 0.0065.

Following the additional contribution of the smooth junction, the calculated length at a gap of 500 nm should be 45 μm rather than 55 μm obtained by the FDE method.

Figure 7 presented the final geometry of the OMT's directional coupler with SOI waveguides and designated monitors.

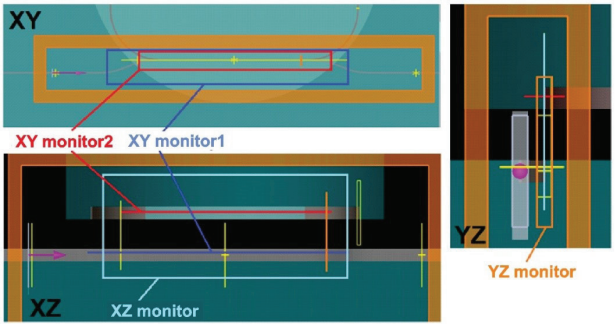

Figure 7 – Geometry of the optical measuring transducer with silicon on insulator waveguides

Figures 8–11 present the distribution of the optical field in the waveguide in corresponding cross-sections obtained by the FDTD method.

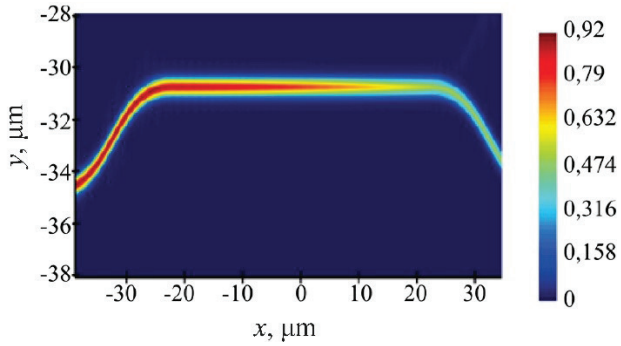

Figure 8 – Distribution of the optical field in the silicon on insulator optical measuring transducer (XY monitor 1)

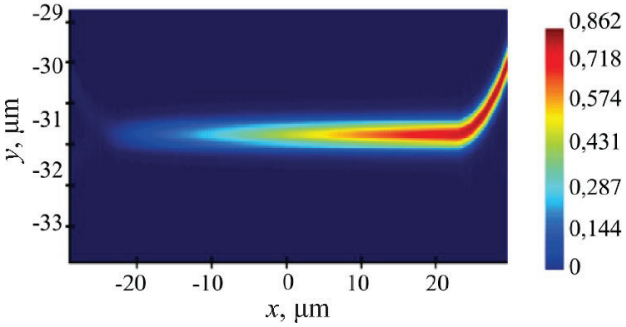

Figure 9 – Distribution of the optical field in the silicon on insulator optical measuring transducer (XY monitor 2)

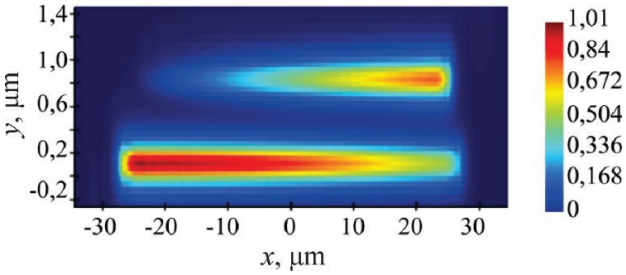

Figure 10 – Distribution of the optical field in the silicon on insulator optical measuring transducer (XZ monitor)

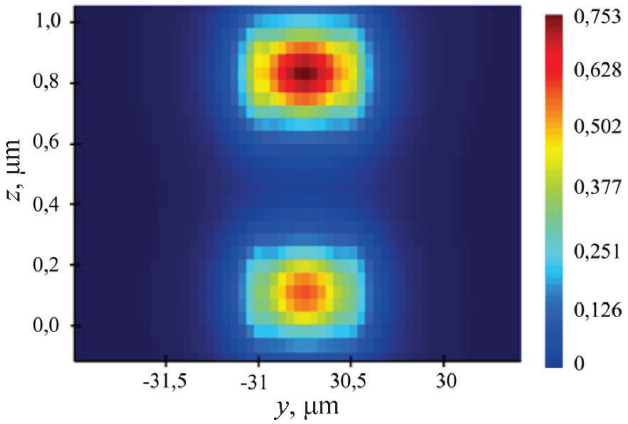

Figure 11 – Distribution of the optical field in the silicon on insulator optical measuring transducer (YZ monitor)

The dependencies of the OMT's transmission coefficient on the gap and wavelength at the selected coupling length were calculated by two methods: FDTD and an analytic method based on the FDE results. This required introducing the dependencies of effective refractive index (n_{eff}) on the wavelength into equation (1):

$$T_{through}(G,\lambda)=\cos^2\left(\frac{\pi\left(n_{eff\,1}(G,\lambda)-n_{eff\,2}(G,\lambda)\right)}{\lambda}L_c\right),$$
$$n_{eff\,1}(G,\lambda)=\left(n_{eff\,1}(G)-n_{eff\,1\lambda 0G0}\right)+a_1+b_1\lambda; \quad (1)$$
$$n_{eff\,2}(G,\lambda)=\left(n_{eff\,2}(G)-n_{eff\,2\lambda 0G0}\right)+a_2+b_2\lambda,$$

where $a_i+b_i\lambda$ is the function of $n_{eff\,i}$ dependence on the wavelength that was calculated by the FDE method at different wavelengths; $n_{eff\ 1\lambda 0G0}$ is the effective index $n_{eff\,i}$ at the gap which was used to calculate the dependence of $n_{eff\,i}$ on the wavelength.

Following the FDTD analysis results, new coupling length values obtained by the FDE method were selected to correspond to the dependencies obtained by the FDTD method (Figures 12–14) for Si_3N_4.

To correspond to the FDTD analysis results, the FDE method results should be increased in terms of the coupling length by 9 μm which corresponds to the increase of the coupling coefficient due to the smooth junction.

Small deviations in the zone of gaps of less than 500 μm are explained by a larger calculation step and insufficiently small grid of finite elements.

The dependencies of the transmission coefficient on the wavelength had identical slopes (Figure 13).

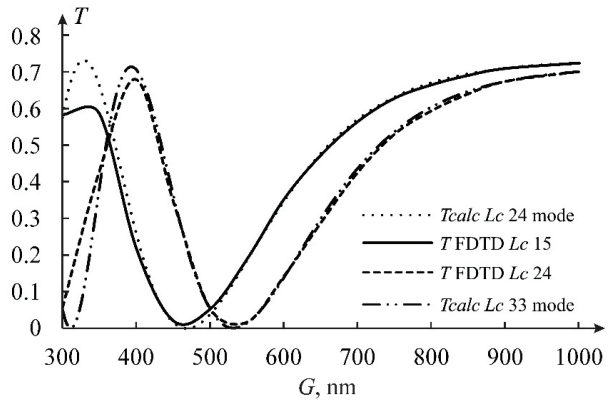

Figure 12 – Comparison of the transmission coefficient dependencies on the gap obtained by the different methods for Si_3N_4

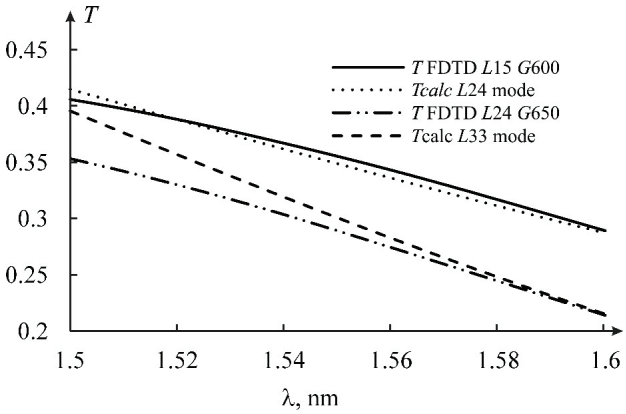

Figure 13 – Dependence of the transmission coefficient on the wavelength for Si_3N_4

Similar analysis was made for the SOI technology and 220×500-nm waveguides (Figures 14–15).

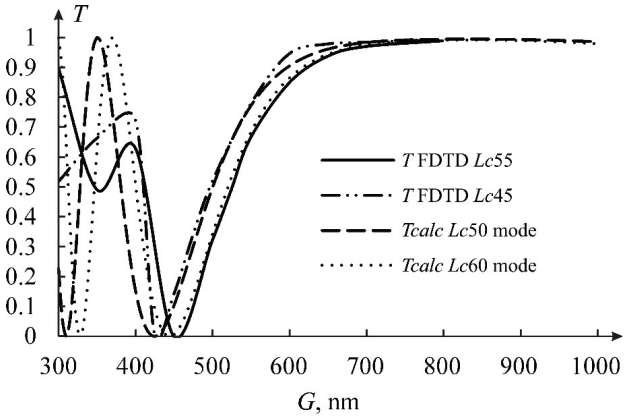

Figure 14 – Comparison of the dependencies of the transmission coefficient on the gap obtained by the different methods for silicon on insulator

To correspond to the FDTD analysis results, the FDE method results should be increased in terms of

the coupling length by 5 μm which corresponds to the increase of the coupling coefficient due to the smooth junction.

Small deviations in the zone of gaps of less than 500 μm are explained by a larger calculation step and insufficiently small grid of finite elements.

The dependencies of the transmission coefficient on the wavelength had identical slopes (Figure 15).

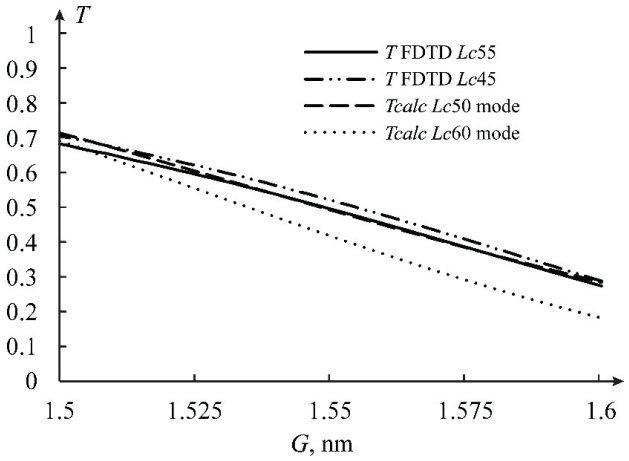

Figure 15 – Dependence of the transmission coefficient on the wavelength for silicon on insulator

The analysis of the OMT's transmission coefficient dependence on the wavelength for both technologies has shown that wavelength can be used for more accurate adjustment and selection of the OMT's working point. Under the variation of the wavelength from 1.5 to 1.6 μm, the transmission coefficients changed from 0.3 to 0.7 for SOI and from 0.2 to 0.4 for Si_3N_4.

The transmission coefficients of the OMT in the linear range of gap variation can be estimated as:

$$K_o = \frac{T_{opt}^{\max} - T_{opt}^{\min}}{G_{\max} - G_{\min}}, \quad (2)$$

where $T_{opt}^{\max}$ and $T_{opt}^{\min}$ are maximum and minimum optical power at the coupler output; $G_{\max}$ and $G_{\min}$ are maximum and minimum gaps between the waveguides.

For the obtained characteristics of the OMT, the calculated transmission coefficients were $5.375 \cdot 10^6$ m^{-1} for SOI wafer and $2.75 \cdot 10^6$ m^{-1} for Si_3N_4. Smaller values of the OMT's transmission coefficient were primarily conditioned by large losses in the waveguide.

Conclusions

The optical measuring transducer for the presented microelectromechanical pressure sensor is characterized by the optical transmission coefficient which–as it was shown–depends on the geometric parameters of the waveguides. Following the results obtained by the computer analysis methods, it was established that the topology of the transducer implementing a directional coupler can be built with gaps of 500 nm in the case of waveguides made of silicon. The calculated minimum bend radius of the waveguide with dimensions of 220×550 nm amounted to 5 μm. The coupling length in this case reached 45 μm. The topology of the transducer for silicon nitride waveguides with dimensions of 350×1400 nm can be built with gaps of 600 nm. As compared to the silicon waveguides, the coupling length of the silicon nitride waveguides amounted to 15 μm, while their minimum bend radius reached 60 μm.

The linearity of the optical transducer characteristics was reached by the selection of the initial inter-waveguide gap. This value lied in the middle of the linear section of the dependence of the optical transmission coefficient on the gap. The linear working section of the dependence lied within 500±80 nm for silicon waveguides and within 600±80 nm for silicon nitride waveguides. The optical transmission coefficient ranged from 0 to 0.86 for silicon waveguides and from 0.09 to 0.53 for silicon nitride waveguides, which corresponded to calculated transmission coefficients of $5.375 \cdot 10^6$ m^{-1} for the former and $2{,}75 \cdot 10^6$ m^{-1} for the latter.

Acknowledgments

The results were obtained with the support of the Ministry of Science and Higher Education of the Russian Federation (theme No. FEWM-2024-0008).

References

1. Bhat KN, Nayak MM. MEMS Pressure Sensors- An Overview of Challenges in Technology and Packaging. Inst. Smart Struct. Syst. J. 2013;2(1):39-71.

2. Barlian AA, Park W-T, Mallon JR, Rastegar AJ, Pruitt BL. Review: Semiconductor Piezoresistance for Microsystems. Proceedings of the IEEE. 2009;97(3):513-552. **DOI:** 10.1109/JPROC.2009.2013612

3. Kanekal D, Jindal SK. Investigation of MEMS Piezoresistive Pressure Sensor with a Freely Supported Rect-

angular Silicon Carbide Diaphragm as a Primary Sensing Element for Altitudinal Applications. Silicon. 2023;(15):1947-1959. **DOI:** 10.1007/s12633-022-02146-z

4. Kyoung-Ho Ha, Heeyong Huh, Zhengjie Li, Nanshu Lu. Soft Capacitive Pressure Sensors: Trends, Challenges, and Perspectives. ACS Nano. 2022;16(3):3442-3448. **DOI:** 10.1021/acsnano.2c00308

5. Yulan Lu, Pengcheng Yan, Chao Xiang, Deyong Chen, Junbo Wang, Bo Xie and Jian Chen. A Resonant Pressure Microsensor with the Measurement Range of 1 MPa Based on Sensitivities Balanced Dual Resonators. Sensors. 2019;19(10):2272. **DOI:** 10.3390/s19102272

6. Shahiri Tabarestani M. Analytical Analysis of Capacitive Pressure Sensor with Clamped Diaphragm. Int. J. Eng. 2013;26(3(C)):297-302. **DOI:** 10.5829/idosi.ije.2013.26.03c.09

7. Boukabache A. [et al.]. Characterization and modelling of the mismatch of TCRs and their effects on the drift of the offset voltage of piezoresistive pressure sensors. Sensors Actuators, A Phys. 2000;84(3):292-296. **DOI:** 10.1016/S0924-4247(00)00406-4

8. Belwanshi V. Analytical modeling to estimate the sensitivity of MEMS technology-based piezoresistive pressure sensor. J Comput Electron. 2021;(20):668-680. **DOI:** 10.1007/s10825-020-01592-5

9. Park S-H, Lee HB, Yeon SM, Park J, Lee NK. Flexible and Stretchable Piezoelectric Sensor with Thickness-Tunable Configuration of Electrospun Nanofiber Mat and Elastomeric. Substrates. ACS Applied Materials & Interfaces. 2016;8(37):24773-81. **DOI:** 10.1021/acsami.6b07833

10. Xu MG, Geiger H, Dakin JP. Fibre grating pressure sensor with enhanced sensitivity using a glass-bubble housing. Electronics Letters. 1996;32(2):128-129. DOI: 10.1049/el:19960022

11. Arkwright JW, Underhill ID, Maunder SA, Jafari A, Cartwright N, Lemckert C. Fiber Optic Pressure Sensing Arrays for Monitoring Horizontal and Vertical Pressures Generated by Traveling Water Waves. IEEE Sensors Journal. 2014;14(8):2739-2742. **DOI:** 10.1109/JSEN.2014.2311806

12. Wang T, Ge Y, Ni H, Chang J, Zhang J, Ke W. Miniature fiber pressure sensor based on an in-fiber confocal cavity. Optik. 2018;(171):869-875. **DOI:** 10.1016/j.ijleo.2018.06.151

13. Guo F, Fink T, Han M, Koester L, Turner J, Huang J. High-sensitivity, high-frequency extrinsic Fabry–Perot interferometric fiber-tip sensor based on a thin silver diaphragm. Optics Letters. 2012;37(9):1505-1507. **DOI:** 10.1364/OL.37.001505

14. Evgenii Barbin, Tamara Nesterenko, Aleksej Koleda, Evgeniy Shesterikov, Ivan Kulinich, Andrey Kokolov and Anton Perin. The Design, Modeling and Experimental Investigation of a Micro-G Microoptoelectromechanical Accelerometer with an Optical Tunneling Measuring Transducer. Sensors. 2024;24(3):765. **DOI:** 10.3390/s24030765